THE MINERALOGY, PETROGRAPHY, MAGNESIUM AND OXYGEN ISOTOPIC COMPOSITIONS OF A WOLLASTONITE-BEARING FUN CAI FROM THE CV CHONDRITE NWA 779. K. Thrane[1*], K. Nagashima[2], A. N. Krot[2] and M. Bizzarro[1]. [1]Geological Museum, University of Copenhagen, Denmark. [2]Hawai'i Institute of Geophysics and Planetology, University of Hawai'i at Manoa, USA. *kthrane@geol.ku.dk

Introduction: Calcium-aluminum-rich inclusions (CAIs) with Fractionation and Unknown Nuclear isotope anomalies (FUN CAIs [1]) are very rare objects reported exclusively in CV carbonaceous chondrites. These include the Allende CAIs *C1* [2,3], *EK1-4-1* [4], *HAL* [5], *CG-14* [6], *DH8*, *B7F6*, *DH10*, and *HB2* [7], and the Vigarano CAI *1623-5* [8]. FUN CAIs are characterized by large mass-dependent fractionation effects in Mg, Si and O, relatively large nucleosynthetic anomalies in several elements (e.g., Ca, Ti, Si, Sr, Ba, Nd, Sm), and low inferred abundance of ^{26}Al. These observations are often interpreted as evidence for formation of FUN CAIs by thermal processing of pre-solar dust aggregates [5] prior to injection and homogenization of ^{26}Al in the solar nebula [9]. If this is correct, FUN CAIs can potentially provide important constraints on the age of the Solar System, composition of the primordial dust in the solar nebula and the earliest stages of its thermal processing.

Most FUN CAIs were discovered and extensively studied 20-30 years ago. These studies consumed most materials of FUN CAIs. To identify new FUN CAIs in CV chondrites suitable for Pb-Pb isotope dating and detailed mineralogical and *in situ* isotope measurements, we initiated a systematic search for coarse-grained igneous CAIs with large mass-dependent fractionation effects in Mg in polished slabs of CV chondrites using multi-collector inductively coupled plasma mass spectrometry (MC ICP-MS) and in polished sections using *in situ* measurements by secondary ionization mass spectrometry (SIMS). Here we report the mineralogy, petrography, magnesium and oxygen isotopic compositions of a newly identified FUN CAI from the CV chondrite NWA 779, named KT-1. This is the first wollastonite-bearing Type B FUN CAI.

Analytical Techniques: A centimetre size piece of NWA 779 (CV3) containing the exposed FUN CAI was mounted in epoxy and polished. The CAI was studied using optical and scanning electron micropscopy (SEM), electron probe microanalysis and SIMS. The sample was mapped in Ca, Al, Mg, Ti, Na, Si, and Cl Kα X-rays with a Cameca SX-50 electron microprobe and studied in backscattered electron mode with the JEOL 5900LV SEM/EDS.

Mg isotopic compositions were measured by both MC-ICPMS and SIMS. The MC-ICPMS analyses was conducted with the aim of getting a sample representative of the bulk inclusion. A hole of ~500 μm in diameter was drilled out (Fig. 1a), corresponding to approximately ca. 0.1 mg of powder. The sample was digested and the Mg was purified by ion exchange chemistry and the Al/Mg and the Mg isotopes were measured by the Axiom MC-ICPMS at the University of Copenhagen following procedures outlined in [10] . Mg isotopes were also measured *in situ* with the Cameca 1280 SIMS at Universty of Hawai'i. A 100–150 pA O^- primary ion beam was focused to ~1-5 μm. The mass-resolving power was set to ~3800, sufficient to separate interfering hydrides and doubly charged $^{48}Ca^+$. Mg isotopes were measured with a monocollector EM. Terrestrial and synthetic standards were used to correct for instrumental mass fractionation (IMF). An exponential mass fractionation law with exponent = 0.514 [11] was used for calculation of excess/deficit of ^{26}Mg.

O-isotopic compositions were measured with the Cameca 1280 SIMS at Universty of Hawai'i in multicollection mode. A focused Cs^+ primary beam of 1.8 nA was used to presputter regions of 25×25 μm^2. The raster size was then reduced and oxygen isotopes were measured from the ~10×10 μm^2 central region. The ^{16}O and ^{18}O ion beams were measured at MRP ~2000 using Faraday cups of multicollector; whereas ^{17}O was measured using EM in monocollector mode at MRP ~5500. IMF effects were corrected by analyzing San Carlos olivine, Burma spinel, and Cr-augite. Melilite and wollastonite compositions, for which standards were lacking, were corrected by assuming their IMF are similar to those of San Carlos olivine and augite, respectively. Uncertainties ~1.5‰ in δ^{17}O and δ^{18}O were estimated from overall standard data obtained during two sessions.

Mineralogy and petrography: KT-1 is 2.5 mm in diameter and consists of chemically-zoned, coarse-grained melilite and fassaite (in wt%, TiO_2, 2-11; Al_2O_3, 19-26) poikilitically enclosing euhedral spinel grains, which are heterogeneously distributed in the CAI (Figs. 1a,b). The coarse melilites are zoned from $Åk_{17}$ in the core to $Åk_{44}$ in the rim; no difference in the composition of the melilites from the interior of the CAI towards the edge is observed. Two interstitial regions between coarse-grained melilite and fassaite consist of fine-grained melilite, anorthite, wollastonite, and Al-diopside, which may represent last crystallizing melt. The inferred crystallization sequence of the CAI is sp → sp+mel → sp+mel+fas → wo+di+mel+an. A region of relatively fine-grained fassaite and melilite occurs near the wollastonite-diopside-melilite-anorthite domain (Fig. 1c), possibly indicating some re-melting of the CAI.

Magnesium isotopic composition: The MC-ICPMS analyses representing the "bulk" sample yielded a δ^{26}Mg* deficit of –0.41 ± 0.02‰ and a δ^{25}Mg of 39.73 ± 0.01‰ (n=6). Individual grains of melilite, spinel, wollastonite and fassaite were analysed *in situ* by SIMS and have a relatively small range of mass fractionation with δ^{25}Mg variying from +36‰ to +41‰ (Fig. 2). The degree of fractionation among spinel, melilite, fassaite, and wollastonite is generally consistent with their inferred crystallization sequence, with fassaite being the most fractionated mineral. No clear excess/deficit of δ^{26}Mg* were identified in KT-1 by SIMS measurements.

Oxygen isotopic composition: The spinel analyses and most of the analyses of coarse-grained fassaite plot along a mass-dependent fractionation line parallel to the Terrestrial Fractionation (TF) line (Fig. 3). The data for fine-grained fassaite, wollastonite and some of the coarse-grained fassaites define a line extending from the mass-dependent fractionation line towards the TF line. The melilite data plot slightly to the right of this line, near its intersection with the TF line.

Discussion: The coarse-grained texture and chemical zoning of coarse melilite and fassaite indicate relatively slow crystallization of the CAI melt. The observed range in O-isotopic compositions of spinel and coarse-grained fassaite defining a mass-dependent fractionation trend must

have resulted from evaporation of such a crystallizing melt. Conversely, the interstitial pockets of fine-grained material composed of wollastonite, diopside, melilite and anorthite appears to represent fast crystallizing residual melt. The spinifex-like texture of the wollastonite-bearing pockets suggest quenching from a melt at 1000-1100°C, possibly as a result of incomplete re-melting during transient heating event(s). Fine-grained fassaite-melilite intergrowths occur near one of the pockets and may also have formed during this melting episode. The latter event appears to have occurred in ^{16}O-poor gaseous reservoir and resulted in incomplete O-isotopic exchange in the melted minerals (fine-grained fassaite, wollastonite, and melilite) defining an exchange line. We note that O-isotopic compositions of melilite throughout the CAI are slightly displaced relative this line, suggesting additional isotopic exchange, possibly during fluid-assisted thermal metamorphism on the CV parent asteroid [12]. The Mg data infer that the evolution in oxygen from ^{16}O-rich to ^{16}O-poor took place before ^{26}Al was injected and homogeneously distributed into the solar nebula.

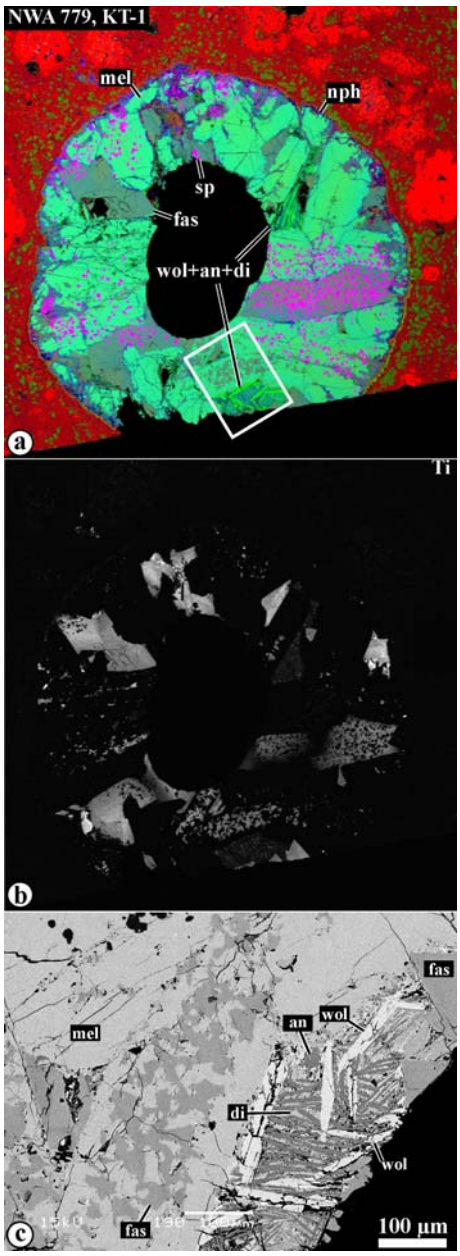

Fig. 1. Combined elemental map in Mg (red), Ca (green) and Al Kα (blue) X-rays (a) and elemental map in Ti Kα of KT-1 (b). Region outlined in (a) is shown in detail in (c). (c) BSE image of the wollastonite (wol) – diopside (di) – anorthite (an) – melilite (mel) region and region composed of fine-grained fassaite (fas) and melilite.

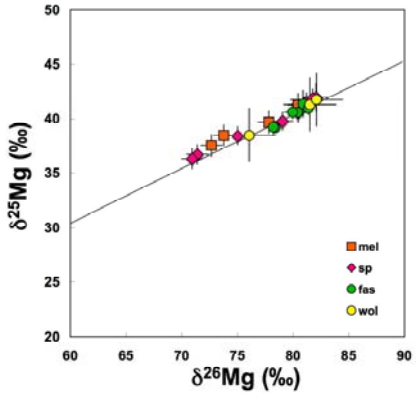

Fig. 2. Mg isotopic compositions in individual minerals in the KT-1. Solid curve is a mass fractionation curve with a mass fractionation exponent of 0.514 [10].

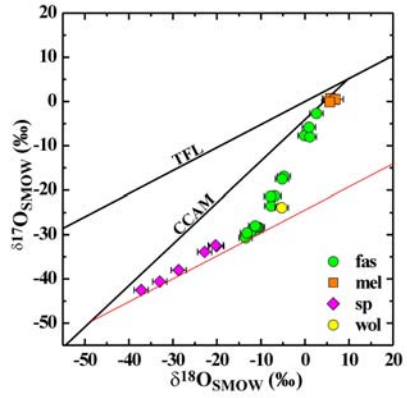

Fig. 3. O-isotopic compositions of individual minerals in KT-1. fas = fassaite; mel = melilite; sp = spinel; wol = wollastonite. TFL = terrestrial fractionation line. EL = exchange line defined by compositions of fassaite only. Red line is mass-dependent fractionation line defined for several Allende FUN CAIs [13].

References: [1] Wasserburg G. J. et al. (1977) *GRL, 4,* 299. [2] Clayton R. N. et al. (1977) *EPSL, 34,* 209. [3] Gray C. M. et al. (1973) *Icarus, 20,* 213. [4] Clayton R. N. & Mayeda T. K. (1977) *GRL, 4,* 295. [5] Lee T. et al. (1980) *GRL, 7,* 493. [6] Clayton R. N. et al. (1984) *GCA, 48,* 535. [7] Brigham C. A. (1990) *PhD Thesis, CalTech.* [8] Davis A. M. et al. (2000) *MAPS, 35,* A47. [9] Sahijpal S. & Goswami J. N. (1998) *ApJ, 509,* L137. [10] Thrane et al. (2007) *ApJ,* 646, L159 [11] Davis A. M. et al. (2005) *LPS, 36,* #2334. [12] Nagashima K. et al. (2007) *LPS, 38,* #2059. [13] Krot A. N. et al. (2008) *LPS,* this vol.